[Frontiers in Bioscience 13, 790-805, January 1, 2008]

Molecular imaging of human epidermal growth factor receptor 2 (HER-2) expression

Gang Niu, Weibo Cai, Xiaoyuan Chen

The Molecular Imaging Program at Stanford (MIPS), Department of Radiology and Bio-X Program, Stanford University School of Medicine, Stanford, California

TABLE OF CONTENTS

1. ABSTRACT

The human epidermal growth factor receptor 2 (HER-2) is a key member of the HER family of receptor tyrosine kinases. Activation of HER-2 affects cell growth, proliferation, migration, adhesion, and survival. Due to its crucial role in carcinogenesis and tumor progression, HER-2 has been intensively investigated as a target for cancer therapy. The ability to quantitatively image HER-2 expression in a noninvasive manner can aid in lesion detection, patient stratification, new drug development/validation, dose optimization, and treatment monitoring. This review summarizes the current state of understanding in multimodality imaging of HER-2 using positron emission tomography (PET), single photon emission computed tomography (SPECT), optical, and magnetic resonance (MR) imaging with HER-2 specific antibodies, antibody derivatives and affibodies as targeting ligands. Successful development of new HER-2 targeted imaging agents with optimal *in vivo* stability, targeting efficacy, and desirable pharmacokinetics for clinical translation will enable maximum benefit in cancer patient management.

2. HUMAN EPIDERMAL GROWTH FACTOR RECEPTOR 2 (HER-2)

Human epidermal growth factor receptor 2 (HER-2) is a cell membrane surface-bound receptor tyrosine kinase. It is also known as ErbB-2 (erythroblastic leukemia viral oncogene homolog 2). HER-2 belongs to the epidermal growth factor receptor (EGFR) family, which comprises of EGFR, HER-2, HER-3, and HER-4. The oncogene encoding HER-2, originally termed as NEU, was derived from rat neuro/glioblastoma cell lines (1). Unlike other members in the HER family, HER-2 is an orphan receptor with no naturally occurring ligand identified to date. After the interaction of ligands (such as EGF, transforming growth factor-alpha (TGF-α), and amphiregulin) with EGFR, HER-3 or HER-4, preferential heterodimerization of these members with HER-2 will occur. The dimerization activates the inherent kinase activity of the protein, thereby promoting the autophosphorylation of tyrosine residues in the cytoplasmic C-terminal region. Consequently, multiple downstream pathways may be activated, including the phosphatidylinositol 3-kinase (PI3K)/AKT and mitogen

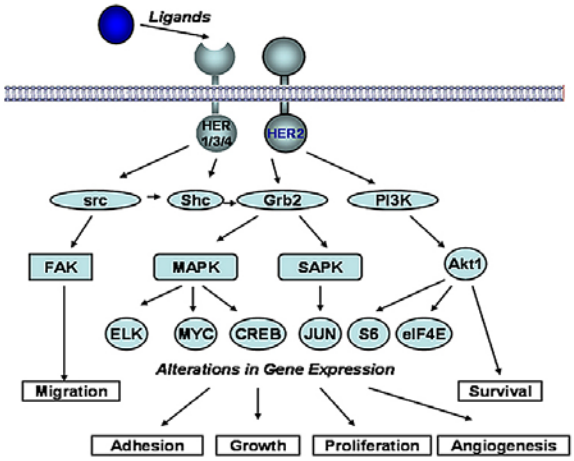

Figure 1. Selected HER-2 signaling pathways. HER-2 can interact with different members of the HER family and activate mitogenic and antiapoptotic pathways. Adapted with permission from ref. 2.

activated protein kinase (MAPK) pathways. Though variations in the activating ligands and the composition of the HER-2 dimers lead to the diversity of downstream signaling, HER-2 activation can affect cell growth, proliferation, migration, adhesion, and survival (Figure 1) (2) .

The HER-2 gene is located at the long arm of human chromosome 17 (17q11.2-q12) and was first recognized as a potent oncogenic mutant in neuroglioblastomas that developed in carcinogen exposed rats (3). HER-2 overexpression increases cell proliferation, anchorage-independent cell growth, cell migration, and invasiveness (4, 5). Hyperactivation of HER signaling pathways is implicated in the proliferation of many cancer cell types. Overexpression of HER-2 has been detected in up to 30% of breast and ovarian cancers (6). High frequency of HER-2 overexpression has also been noted in other common types of cancers, including prostate, lung, gastric, and oral cancers (7-9). In addition, overexpression of HER-2 has been correlated with invasive and poor prognostic features, and it is often associated with shorter patient survival, early relapse, and an increased number of lymph node metastases (10). Importantly, overexpression of HER-2 has been implicated in mediating increased resistance to chemotherapeutic agents. Due to its crucial role in carcinogenesis and tumor progression, HER-2 has been intensively investigated as a target for cancer therapy.

One strategy of targeted cancer therapy against HER-2 is to use monoclonal antibodies (mAbs). Trastuzumab (Herceptin, Genentech, Inc., San Francisco, CA), approved by the Food and Drug Administration (FDA) in 1998, was developed by fusing a potent murine monoclonal antibody 4D5 that interacts with the extracelluar domain of HER-2 and the framework of human IgG (11). The anti-tumor activity of trastuzumab is mediated through the down-regulation of HER-2 expression (12), blocking heregulin induced activation of HER-2/HER-3 complexes, and inducing the cyclin-dependent kinase 2 inhibitor p27 and Rb-related protein p130 (13). Trastuzumab also sensitizes tumor cells to the effects of tumor necrosis factor (TNF) (14) and the cytotoxic effects of chemotherapeutic agents in some models (13). In women with HER-2-positive metastatic breast cancer, trastuzumab is well tolerated and clinically active as a single agent or in combination with chemotherapy (15).

Another HER-2-targeted monoclonal antibody is pertuzumab (Omnitarg, rhu mAb-2C4, Genentech). Pertuzumab sterically hinders the recruitment of HER-2 into HER ligand complexes and blocks HER-2 homo/heterodimerization with other HER family members (16). Trastuzumab increased pertuzumab-mediated disruption of HER-2 dimerization with EGFR and HER-3. Synergistic effect has been observed with trastuzumab and pertuzumab in inhibiting the survival of BT474 cells (17).

The other approach of anti-HER-2 therapy is to use tyrosine kinase inhibitors (TKIs). Lapatibib is a reversible HER-2 TKI currently in advanced clinical trials. Concentration-dependent anti-proliferative effects of lapatinib have been observed in various breast cancer cell lines. The response to lapatinib was found to be significantly correlated with HER-2 expression (18). Other strategies targeting HER-2 include the use of heat shock protein 90 (Hsp90) inhibitors (e.g. 17-Allylaminogeldanamycin) (19) and HDAC inhibitors (20), targeting HER-2 mRNA through ribozymes (21), antisense, and small interfering RNA (22).

3. MOLECULAR IMAGING OF HER-2 EXPRESSION WITH ANTIBODY DERIVATIVES AND AFFIBODIES

In breast carcinomas, gene amplification is the key event for HER-2 overexpression, whereas no mutation or genetic recombination has been described in human tumors (23). The effectiveness of HER-2 targeted therapy either by antibodies or TKIs is therefore highly dependent on the ability to accurately evaluate the HER-2 status in tumors. Guidelines of The American Society of Clinical Oncology (ASCO) recommend evaluation of HER-2 expression on every primary breast cancer either at the time of diagnosis or at the time of recurrence (24). Analyzing the overexpression or gene amplification of HER-2 in surgical specimens is most commonly accomplished by either immunohistochemical (IHC) staining or fluorescence *in-situ* hybridization (FISH) testing (25, 26).

Currently, various non-invasive molecular imaging modalities are under intensive investigation to provide comprehensive diagnostic information that can improve patient management. Molecular imaging employs contrast agents to detect biomarkers such as growth factor receptors, protein kinases, cell adhesion molecules, proteases, as well as biological processes such as hypoxia, apoptosis, and angiogenesis (27). One of the main goals of molecular imaging is to meet the rapid development of personalized or targeted cancer therapy, which works by tailoring a patient's treatment to the unique set of molecular

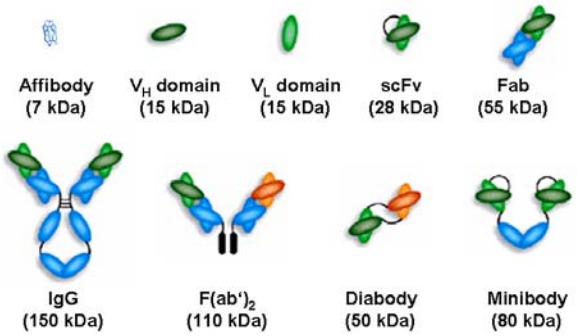

Figure 2. Engineered antibody fragments and Affibody used for imaging HER-2 expression. Adapted with permission from ref. 29.

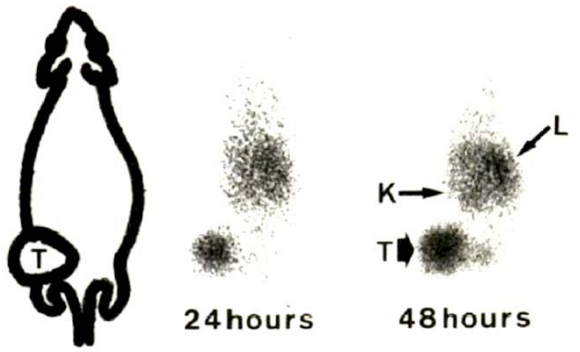

Figure 3. Scintigrams of a nude mouse bearing the A4 xenograft. Images were obtained at 24 and 48 h after the injection of ^{111}In-labeled SV2-61r. T, tumor; L, liver; K, kidney. Adapted with permission from ref. 32.

aberrations driving his/her disease (28). The available modalities include optical imaging, contrast-enhanced ultrasound (CEU), magnetic resonance imaging (MRI), and radionuclide imaging (PET and SPECT).

Antibodies against HER-2 are in the mainstream of the development of therapeutic agents to treat cancers with HER-2 overexpression. Consequently, radiolabeled or other imaging label conjugated antibodies are the most common probes for HER-2 detection. Along the progress from murine monocolonal antibodies, humanized antibodies and antibody fragments, to engineered antibodies (scFv, diabody and minibody) and affibody (Figure 2) (29), in this review, we will focus on imaging HER-2 expression with various molecular imaging modalities, including SPECT, PET, MRI and optical imaging with these antibody, antibody fragment, and affibody based probes.

3.1. Murine monoclonal antibodies

The production of monoclonal antibodies recognizing tumor-associated antigens is made possible by the development in hybridoma technology. These antibodies provide new approaches for the radioimmunoimaging (RII) and radioimmunotherapy (RIT) of cancers and metastases (30). The localization of antibody in tumors following passive transfer of antibodies is governed by a complex series of events involving extravasation of antibody and its diffusion into the tumor tissue. The deposition of an antibody is also dependent on the tumor mass and its location, the binding affinity to tumor-associated antigens, the degree of expression of the relevant antigen, and its stability on tumor cells (31).

Radionuclide imaging techniques include single photon emission computed tomography (SPECT) and positron emission tomography (PET), both of which are highly sensitive. SPECT uses low energy γ-emitting isotopes (e.g. ^{123}I, ^{111}In, and ^{99m}Tc) and is relatively inexpensive and widely available. For imaging purposes, a target-to-nontarget ratio of >1.5 is sufficient for SPECT, whereas planar imaging requires much higher ratios. The first HER-2 specific imaging study was performed in 1991 with a class-switched murine monoclonal antibody SV2-61r that recognizes the extracellular domain of HER-2 (32). ^{111}In labeled SV2-61r through DTPA chelator specifically bound to various adenocarcinoma cells and HER-2 stably transfected NIH-3T3 cells (A4 cells). Intravenously injected ^{111}In-DTPA-SV2-61r localized well to A4 cells xenografted in nude mice (Figure 3). Monoclonal antibody ICR12 is a rat IgG_{2a} with high affinity for an external epitope on the protein core of HER-2 (33, 34). RIT with ^{131}I labeled ICR12 in athymic mice bearing MDA-MB-361 human breast cancer xenografts showed growth inhibition for >24 days at a dose of 600 μCi/mouse (33, 35). A ^{99m}Tc labeled ICR12 had 20 % ID/g tumor uptake, four times greater than that in normal tissues, based on biodistribution study in a mouse model system. In patients selected by IHC staining, planar and SPECT imaging with this ^{99m}Tc-ICR12 showed good tumor localization in both the primary lesion and regional node metastases (36). Scintigrams with ^{99m}Tc-labeled another murine monoclonal antibody CIBCgp185 also showed high radiolabel uptake by the BT474 tumor tissue in mice (37).

ImmunoPET is based on annihilation coincidence detection after labeling a mAb or mAb fragment with a positron-emitting radionuclide. Compared with SPECT, PET has the advantages of higher sensitivity and versatility. Moreover, it is also capable of scatter correction. PET imaging with ^{124}I-labeled ICR 12 has been performed, and MDA-MB-361 tumor xenografts in nude mice of 6 mm diameter could be visualized at 24, 48 and 120 hr after probe injection (38). More PET studies have been carried out with humanized antibody trastuzumab, which will be summarized later.

In comparison with radionuclide imaging, the intrinsic sensitivity of MRI is rather low. Significant signal amplification can be achieved when the contrast agent accumulates in the target cells by passive endocytosis, or by an active transporter system. Gadolinium (Gd)-based contrast agents provide strong positive T1 contrast and a stable complex can be easily formed between Gd and a chelating agent such as DTPA. However, for antibody conjugation, only a limited number of functional groups can be conjugated to the mAb without reducing its binding affinity. Thus, the concentration of contrast agent achieved

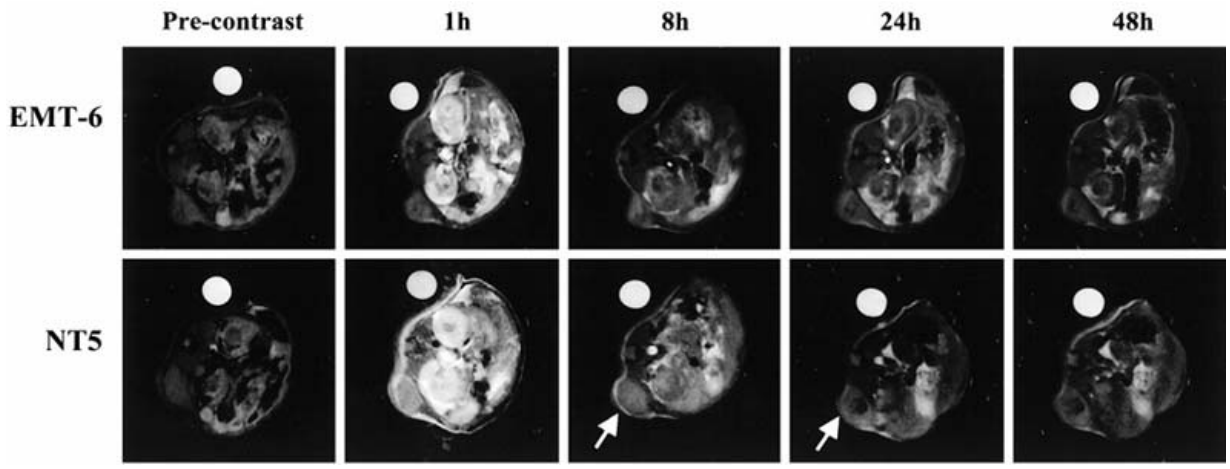

Figure 4. MR T1 weighted images of control EMT-6 (HER-2 negative) and NT-5 tumors obtained before administration of the contrast agent (avidin-GdDTPA conjugate) and at 1, 8, 24, and 48 h after contrast. Tumors were prelabeled with specific biotinylated anti-HER-2 antibodies. Arrows show enhanced signal from the tumor at the 8 and 24 h time points for the HER-2-expressing NT-5 tumor. Adapted with permission from ref. 41.

by direct labeling of the mAb is low and usually not sufficient to generate detectable MR contrast (39). Pre-targeting is one alternative to overcome this obstacle (40). After prelabeled with a biotinylated murine monoclonal IgG1 anti-HER-2 antibody (Ab-9; Clone B10; NeoMarkers) to NT-5 HER-2-expressing cells, positive T1 contrast could be imaged by MRI by the specific binding of avidin-gadolinium complexes. Intensity enhancement was observed in NT-5 cells *in vitro* and in a NT-5 cancer model *in vivo* (Figure 4). However, the maximal signal intensity ratio between HER-2 positive tumors and negative tumors was below 2, which might be due to passive targeting caused by the leaky tumor vasculature (41). Small iron oxide (magnetite) nanoparticles are superparamagnetic, and they have significantly larger magnetic moment than paramagnetic compounds. Monocrystalline iron oxide nanoparticles (MION) have been conjugated to a mouse monoclonal antibody against HER-2. All receptor-positive cell lines, but not the controls, showed strong changes in T2 signal intensity at 1.5 T. However, there is no *in vivo* data available (42).

3.2. Humanized antibodies

The clinical utility of rodent monoclonal antibodies is limited by their immunogenicity and often inefficient secondary immune functions. These issues also hinder the application of murine antibodies in repetitive imaging. Humanized antibodies are commonly created by transplanting the antigen binding segments, known as complementarity determining regions (CDRs), from rodent antibodies into human antibodies (43). The murine mAb 4D5, directed against the extracellular domain of HER-2, is a potent inhibitor of growth of human breast cancer cells that overexpress HER-2 (44). By inserting the CDRs of mAb 4D5 into the framework of a consensus human IgG, a recombinant humanized anti-HER-2 monoclonal antibody called trastuzumab has been developed. Trastuzumab has a higher affinity for HER-2 (K_d = 0.1 nM) than the murine MAb 4D5 (K_d ~ 6 nM), and retains a cytostatic growth inhibitory effect against human breast carcinoma SK-BR-3 cells overexpressing HER-2 (45). Trastuzumab is the first monoclonal antibody approved by the FDA for use in women with breast cancer who have tumors that overexpress HER-2 protein. Trastuzumab has also been used in RIT for tumor control after being labeled with β-particle emitters such as ^{131}I ($t_{1/2}$ = 8.1 d) and ^{186}Re ($t_{1/2}$ = 3.7 d) and α-emitter ^{90}Y ($t_{1/2}$ = 2.7 d) (46, 47). These applications all require accurate evaluation of HER-2 expression status. Trastuzumab has been labeled with various isotopes, chromophores, and paramagnetic nanoparticles for multimodality imaging of HER-2 expression.

Pertuzumab (Omnitarg) is another humanized antibody derived from murine antibody 2C4. In contrast to trastuzumab, pertuzumab sterically blocks HER-2 dimerization with other HER receptors and blocks ligand-activated signaling from HER-2/EGFR and HER-2/HER-3 heterodimers (16). After labeling with the therapeutically interesting β-emitter ^{177}Lu ($t_{1/2}$ = 6.71 d, β^- = 496 keV, γ = 208 keV) through the chelator CHX-A"-DTPA, both direct tissue sampling and gamma camera imaging showed extensive tumor uptake (48).

With DTPA as a chelator at 1:1 molar ratio, trastuzumab was radiolabeled with ^{111}In. The immunoreactive fraction of the purified ^{111}In-DTPA-trastuzumab was 0.87, determined by an SKOV-3 cell-binding assay. HER-2-positive SKOV-3 tumor was clearly visualized on gamma camera scintigram imaged 72 h after injection of ^{111}In-DTPA-trastuzumab (49). In metastatic breast cancer patients (n=15), ^{111}In-DTPA-trastuzumab scintigraphy failed to predict trastuzumab-related cardiotoxicity. However, previously unidentified lesions were visualized in 13 of the 15 patients on the first scans, and the overall detection rate of tumor lesions was 45% at the single-lesion level. The relatively low detection rate may relate to the different size and location of tumors, and

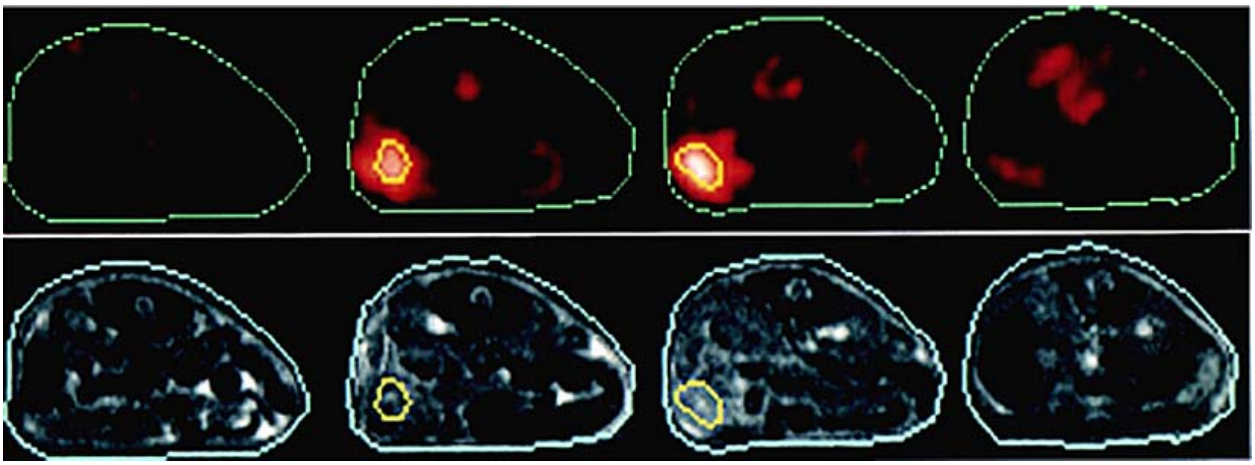

Figure 5. High-resolution transverse MR image slices, registered to corresponding microPET slices. Contours depicting outer periphery of mouse and also collection of tumor nodules near spleen are shown. Adapted with permission from ref. 54.

different HER-2 expression levels between separate metastatic lesions within a patient (50). The α-particle emitter, ^{90}Y, is one of the most frequently used radionuclides for targeted radionuclide therapy (51). Biodistribution of ^{90}Y for dosimetry calculations is typically obtained by imaging using the surrogate radiometal ^{111}In because ^{90}Y does not emit photons. ^{111}In has an almost identical half-life as ^{90}Y, emits 2 γ-rays of 171 and 245 keV, and can be readily incorporated into the same metal chelating agents as ^{90}Y. For these reasons, ^{111}In has been considered an excellent analog for ^{90}Y. However, it has been reported that ^{111}In-trastuzumab did not parallel the uptake of ^{86}Y-trastuzumab in the bone, and thus may not accurately predict the level of ^{90}Y accumulation in the bone for clinical RIT applications (52, 53). Subtle differences in radionuclide retention of the metal chelating agents used for ^{111}In and ^{90}Y mAb labeling can result in a differential release between the two radiometals. With less stability than ^{111}In-DTPA, transchelation of ^{90}Y from the chelating agent can result in a higher dose to the bone and bone marrow, which would not be anticipated from biodistribution data derived from ^{111}In, possibly leading to underestimation of the radiation dose to bone marrow. Thus, quantitative information offered by PET through ^{86}Y radiolabels could enable more accurate absorbed dose estimation for ^{90}Y RIT (53). Trastuzumab has been labeled with ^{86}Y using 2-(4-isothiocyanatobenzyl) DTPA (SCN-CHX-A-DTPA) as chelator to assess the therapeutic potential of ^{90}Y-trastuzumab in a human ovarian carcinoma (SKOV-3) model. Intra-peritoneal injection of 12–18 MBq of ^{86}Y- trastuzumab led to rapid blood-pool uptake (5-9 h) followed by tumor localization (26-32 h), as confirmed by co-registered MR images (Figure 5) (54).

Besides the radionuclides, chelators used in the labeling process may also affect the biodistribution of imaging agents. Charged linkers such as (4-isothiocyanatobenzyl-ammonio)-undecahydro-closo-dodecaborate (DABI) and N-succinimidyl 5-(tributylstannyl)-3-pyridinecarboxylate have been used to label trastuzumab with a positron emitter ^{76}Br ($t_{1/2}$ = 16.2 h) (55, 56). These studies were intended to improve the intracellular retention of the radioactive label after internalization and degradation of targeting proteins. However, *in vitro* SKOV-3 cell binding test revealed that radiobromination of trastuzumab using N-succinimidyl 5-bromo-3-pyridinecarboxylate did not improve the cellular retention of radioactivity compared to using N-succinimidyl 4-bromobenzoate (56).

Trastuzumab has also been labeled with paramagnetic or superparamagentic agents for MRI imaging. Superparamagnetic iron oxide (SPIO) particles generate significant susceptibility changes, resulting in strong T2 and T2* contrast. When internalized by cells, SPIO particles enable single-cell MR detection on microscope slides (57). Magnetic Active Compensation System (MACS) Streptavidin Microbeads (Miltenyi Biotec, Auburn, CA) are 50 nm diameter nanoparticles containing a SPIO core coated with a polysaccharide layer (55–59% iron oxide w/w). The commercially available streptavidin-conjugated superparamagnetic nanoparticles generated strong T2 MR contrast in Her-2-expressing cells prelabeled with biotinylated trastuzumab. The contrast observed in MR images was proportional to the expression level of HER-2 determined independently with FACS analysis. Unfortunately, there is no *in vivo* imaging data available (58). Lee *et al.* (59) has developed magnetism-engineered iron oxide (MEIO) nanoparticles, which possess high and tunable magnetism. These MEIO nanoparticles were conjugated with maleimide-activated trastuzumab. *In vitro* cell studies showed that as the relative HER-2 expression level increased, the MR contrast increased consistently. *In vivo* imaging with a dose of 20 mg/kg in NIH3T6.7 tumor-bearing nude mice enabled MR detection of tumors with relatively small size. Both SPIO and MEIO are T2 contrast agents. The resulting dark signal may mislead the clinical diagnosis in T2-weighted MRI because the signal is often confused with the signals from bleeding, calcification, or metal deposits, and the susceptibility artifacts distort the background image (60). A T1 MRI contrast agent using MnO nanoparticles has been synthesized and encapsulated

in a polyethyleneglycol (PEG)-phospholipid shell to make them biocompatible. After conjugation with trastuzumab, the functionalized MnO nanoparticles were delivered and accumulated at the site of breast cancer in a nude mice model. However, the specificity of the imaging target needs to be confirmed further (61).

Optical imaging techniques have already been developed for *in vitro* and *in vivo* applications in molecular and cellular biology. However, optical imaging methods suffer from limited tissue penetration, which limits them to small animal models and precludes their application in a non-invasive human imaging system (62). Fluorescent dye Cy5.5 was coupled to trastuzumab and tested in both SK-BR-3 (HER-2 positive) and PE/CA-PJ34 (HER-2 negative) tumor models. It was found that the relative fluorescence intensities in SK-BR-3 tumors were only slightly higher than those in PE/CA-PJ34 tumors at 16-24 h after probe administration (63). Compared with conventional organic dyes, quantum dots (QDs) have several advantages, such as narrow, symmetrical and tunable emission spectra, excellent photostablility, and broad absorption spectra (64). Wu *et al.* (65) have coated organic-soluble, CdSe/ZnS core-shell nanocrystals with octylamine-modified polyacrylic acid. The coated QDs were then linked to a mouse anti-HER-2 antibody to label HER-2 on the surface of fixed and live cancer cells. Using QDs with different emission spectra conjugated to HER-2 and streptavidin, they simultaneously detected two cellular targets with one excitation wavelength (65).

Nanoshells are optically tunable nanoparticles that consist of a dielectric core surrounded by a thin gold shell. In contrast to conventional organic dyes, nanoshells have continuous and broad wavelength tunability, far greater scattering and absorption coefficients, increased chemical stability, and improved biocompatibility. Nanoshell bioconjugate with anti-HER-2 antibody could be used to target live human breast carcinoma cells overexpressing HER-2 (66). Moreover, immunotargeted nanoshells can be engineered to both scatter and absorb light in the near-infrared (NIR; 700-900 nm) region, which enables both optical molecular cancer imaging and selective destruction of targeted carcinoma cells through photothermal therapy. In an *in vitro* experiment, dual imaging/therapy immunotargeted nanoshells were used to detect and destroy breast carcinoma cells overexpressing HER-2 (67). Overall, however, optical imaging is still mainly limited to the *in vitro* cell culture applications, and the practicability of these approaches *in vivo* needs further investigation.

3.3. Antibody fragments

The large molecular size of intact antibodies leads to prolonged serum half-life. Intact antibodies also take a long time for maximal dose deposition in the target tissue, due to the slow diffusion from the vasculature into the tumor (68). Moreover, IgG intratumoral diffusion is limited by its size to a penetration rate of about 1 mm every 2 days, potentially resulting in heterogeneous deposition in tumor (69). Tailoring the antibody molecules by enzymatic digestion, antibody fragments $F(ab')_2$ and Fab may allow more rapid elimination from the blood and normal tissues (except kidneys), due to the smaller size than intact antibodies (70). However, these antibody fragments are tedious to prepare and not readily reproducible (71). Following modification with 6-hydrazinonicotinic (HYNIC) N-hydroxysuccinimide ester, the trastuzumab Fab was labeled with ^{99m}Tc to image HER-2-overexpressing human breast cancer BT-474 xenografts in athymic mice. Although modification with approximately two molecules of HYNIC diminished its receptor-binding affinity by four fold, ^{99m}Tc-trastuzumab Fab localized in BT-474 xenografts and tumors could be visualized at 6 and 24 h post-injection. The tumor uptake and tumor-to-background ratio for ^{99m}Tc-trastuzumab Fab were significantly higher than those for ^{99m}Tc-labeled control irrelevant anti-CD33 HuM195 Fab (72). The trastuzumab Fab were also radioloabeled with ^{111}In after DTPA derivatization, and the binding affinity was not significantly decreased with a dissociation constant (K_d) that changed from 14-36 to 47. ^{111}In-trastuzumab Fab localized specifically in HER-2-positive BT-474 human breast cancer xenografts in athymic mice (compared with ^{111}In-HuM195 anti-CD33 Fab). BT-474 tumors as small as 3-5 mm in diameter could also be imaged as early as 24 h post-injection (73).

A direct comparison between Fab and full length antibody has been reported with ^{111}In labeled trastuzumab and a trastuzumab-derived Fab (Fab4D5) through DOTA conjugation (74). In a spontaneous mammary tumor model in MMTV/HER-2 transgenic mice, ^{111}In-DOTA-Fab4D5 showed early tumor localization at 2 h with little retention followed by rapid accumulation in the kidneys by 6 h, which indicated a rapid washout of Fab from the tumor after initial accumulation. ^{111}In-DOTA-trastuzumab was slow to accumulate in tumors and slow to clear from normal tissues, and significant tumor deposition was achieved by 24 h. The peak tumor uptake for Fab was around 12 % ID/g at 16 hr post-injection and around 45 % ID/g at 24 hr post-injection for trastuzumab. By introducing an albumin binding sequence to Fab4D5, a bifunctional molecule AB.Fab4D5 capable of binding albumin and tumor antigen HER-2 simultaneously has been developed (75). ^{111}In-DOTA-AB.Fab4D5 targeted tumors more rapidly and quickly cleared from blood, leading to a lower overall normal tissue exposure. Unlike Fab4D5, AB.Fab4D5 did not accumulate in the kidneys, suggesting that association with albumin led to an altered route of clearance and metabolism. Remaining bound to albumin makes the apparent molecular weight of AB.Fab4D5 closer to that of trastuzumab (68 + 52 = 120 versus 150 kDa) than that of Fab4D5 (50 kDa). Still, the shape and slightly reduced size of the albumin/AB.Fab4D5 complex may allow for preferential diffusion relative to the full-length IgG (74).

Despite preselection for HER-2 overexpression based on IHC staining or FISH of a tumor biopsy, only 11–35% of patients in phase II trials responded to the drug when it was given as a single agent (76). Thus, assessment of the early response to trastuzumab therapy can improve patient care by identifying patients who may not benefit

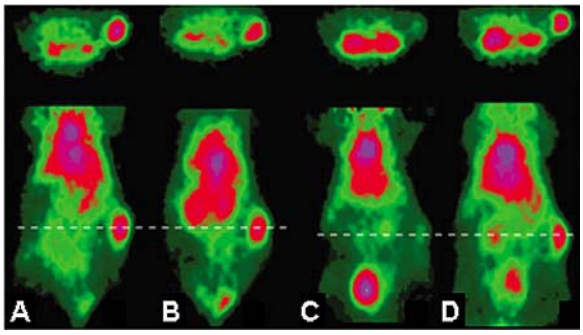

Figure 6. MicroPET images (coronal slice and transverse slice through tumor and kidneys) of two different nude mice with single BT-474 tumors. (A) A mouse at 3 h after injection with ^{68}Ga-DOTA-F(ab')$_2$-trastuzumab and before 17-AAG treatment. (B) The same mouse after it had received 3 ✕50 mg/kg of 17-AAG and rescanned 24 h later. (C, D) Comparable images of a control mouse 3 h after one dose of ^{68}Ga-DOTA-F(ab')$_2$-trastuzumab (C) and after a second dose 24 h later (D). Adapted with permission from ref. 77.

from such targeted molecular therapy. It will be helpful to avoid unnecessary toxic side effects by timely switching to a different, and more effective therapeutic approach. Smith-Jones *et al.* (77) labeled F(ab')$_2$ fragment of trastuzumab with a positron emitter ^{68}Ga ($t_{1/2}$ = 68 min) to assess the degradation of HER-2 by 17-allylaminogeldanamycin (17-AAG), a heat shock protein 90 (Hsp90) inhibitor. Taking advantage of the fast blood clearance of F(ab')$_2$ and quick decay of ^{68}Ga, they repetitively imaged HER-2 expression at 24 h intervals. Based on the microPET quantification , HER-2 expression was reduced by almost 80% in the animals 24 hrs after 17-AAG treatment (Figure 6) (77). In a follow-up study, tumor response to 17-AAG treatment were assessed by ^{68}Ga-DOTA-F(ab')$_2$-trastuzumab and ^{18}F-FDG PET. Within 24 h after treatment, a significant decrease in HER-2 was measured by HER-2 PET, whereas ^{18}F-FDG PET uptake was virtually unchanged. The 17-AAG treated animals had a reduced uptake of ^{68}Ga-F(ab')$_2$-trastuzumab that lasted until 5 d after treatment, although notable growth inhibition occurred only by 11 d after treatment. The ^{18}F-FDG PET imaging data revealed no significant differences in ^{18}F-FDG metabolism between treated and control group at any of the time points examined. This indicates that HER-2-PET with ^{68}Ga-DOTA-F(ab')$_2$-herceptin could provide accurate information for tumor early response to 17-AAG treatment (78).

3.4. Single chain Fv, diabodies and minibodies

Antibody engineering has made it possible to tailor antigen-binding domains into a single polypeptide with a much smaller size than intact immunoglobulin. A single-chain Fv (scFv) recombinant protein for a given monoclonal antibody can be prepared by connecting genes encoding for heavy-chain and light-chain variable regions at the DNA level by an appropriate oligonucleotide linker. The resulting translation product forms a single polypeptide chain with a linker bridging the 2 variable domains. scFv molecule based on an anti-HER-2 monoclonal antibody 741F8 has been produced in E. coli and radiolabeled with ^{125}I and ^{131}I by chloramine-T method. As expected, the scFv monomer exhibited rapid clearance from blood in SCID mice bearing SKOV-3 tumor xenografts (79).

Compared with intact parental antibody (150 kDa), scFv (25 kDa) for a given immunoglobulin exhibits faster clearance kinetics and deeper tumor penetration; however, the absolute dose deposition of scFv is much lower (80). This is primarily due to its monovalent binding nature, which results in lower functional avidity. The degree and specificity of tumor localization of scFv can be improved by increasing the affinity to its corresponding antigen. By creating mutant scFv gene repertoires and displaying their encoded proteins on the surface of filamentous bacteriophage, affinity mutants of a human scFv (C6.5) that bind to an epitope on the extracellular domain of HER-2 has been created (81). The scFv mutants differ from one other by one to three amino acids, bind to the same HER-2 epitope, and span a 320-fold range of affinities. After iodination, biodistribution studies were performed in SCID mice bearing established SKOV-3 tumors. At 24 h after injection, tumor retention of the highest affinity scFv was 7-fold greater than that of a mutant with 320-fold lower affinity (81). However, the potential impact of affinity on the successful targeting and retention of antibodies and antibody derivatives in tumors remains controversial. One theory postulates that high affinity mAb will not successfully penetrate deeply into tumors due to a binding site barrier effect, in which interaction with the first antigen encountered at the periphery of the tumor will block further diffusion of the mAb into the tumor (82). On the other hand, there is also evidence showing that increased affinity prolonged the tumor retention of radiolabeled antibody (83). A likely explanation is that affinity was not the only variable affecting the tumor localization properties. Other factors, such as accessibility and quantity of the targeted epitopes, might have influenced the results (84).

Divalent and multivalent scFvs (diabodies or tribodies) can result either from the spontaneous dimerization or covalent association of 2 or more monovalent scFvs (85, 86). With their bivalent or multivalent binding, they exhibit better tumor deposition than their scFv counterparts, yet clear faster from circulation than intact antibodies because of their smaller molecular size (55 kDa or 80 kDa) (87). These recombinant antibody fragments with di- or multivalent binding with intermediate molecular weight (60–120 kDa) are a compromise between slow-clearing high-localizing immunoglobulins and fast-clearing low-localizing monovalent scFvs (88). A slightly slower clearance was observed with the divalent 741F8 (sFv')$_2$ comprising a pair of 741F8 sFv with a C-terminal Gly4Cys joined by a disulfide bond (86). Following intravenous administration, both monovalent and divalent forms of 741F8 scFv were specifically retained by SKOV-3 tumors. Compared to a monovalent 741F8 Fab fragment of approximately the same size, the divalent bismalimidohexane-linked 741F8 (sFv')$_2$ showed significantly greater tumor localization. This suggests that the increased avidity of the (sFv')$_2$ was a

factor in its improved tumor retention (14, 79). For direct iodination, it has been noted that even under very mild oxidizing conditions, some proteins lose a portion of their biologic activity, most likely from oxidation of thiols or from iodination of a tyrosine that was involved in the binding. Moreover, iodination of tyrosine residues or agents with a similar structure tends to be recognized and dehalogenized *in vivo* by deiodinases. Instead of direct iodination by Chloramine-T method, 741F8-1 $(sFv')_2$ has also been radioiodinated by using N-succinimidyl p-iodobenzoate (PIB), a protein radioiodination acylating agent. The PIB method involves the coupling of the radioiodine to a nonphenolic aromatic ring of the PIB reagent that is not susceptible to *in vivo* dehalogenase activity. The ^{125}I-PIB complex is then conjugated to lysine residues on the scFv through the formation of an amide bond (89). This method leads to high retention of the radiolabel on the protein and results in prominent tumor localization in tumor-bearing SCID mice (90).

With a small animal phantom, the recovery coefficients were theoretically calculated and applied to the maximum sphere activity concentration measured from the PET images that were acquired by a GE Discovery LS PET/CT System. The recovery coefficients were then applied to quantitative analysis of PET images of SKOV3 tumor-bearing SCID mice using ^{124}I ($t_{1/2}$ = 4.2d) labeled C6.5 diabody. The tumor percentage injected dose per gram estimated from the murine PET image correlated well with those obtained from tissue sampling studies. These results demonstrated the feasibility of performing quantitative PET imaging using a large-bore clinical scanner, which enables high-throughput studies to evaluate the performance of PET tracers by imaging multiple animals simultaneously (91). Animals imaged 4, 8, 24, and 48 hours post-injection of ^{124}I-C6.5 diabody showed that targeting of the radiotracer to the SKOV-3 tumor xenografts peaked at 4 hr pi. However, dehalogenation of the radiotracer resulted in significant uptake of iodine by the thyroid and stomach. C6.5 diabody has also been labeled through a water-soluble form of Bolton-Hunter reagent sulfosuccinimidyl-3-(4-hydroxyphenyl) propionate (SHPP) to avoid dehalogenaton. Animals receiving SHPP-labeled diabody contained lower levels of free iodine in their blood than animals receiving iodogen-labeled diabody. However, the SHPP methodology decreased the immunoreactive fraction of the diabody about 2-fold compared with the iodogen labeling methodology. Moreover, PET images of animals injected with ^{124}I-SHPP-C6.5 diabody exhibited an overall increase in background signal due to residualization of the SHPP moiety (92).

The fusion proteins of scFv with the hinge region and C_H3 domain of immunoglobulin molecule are called minibodies. The hinge region facilitates dimerization mediated by disulphide bond formation and imparts flexibility to the antigen-binding domain. With the molecular weight of 80 kDa, minibodies persist longer than diabodies in the serum, hence allowing higher dose deposition in the tumors (93). Both hingeless minibody and hinge-minibody have been constructed by fusing scFv of an internalizing HER-2 10H8 monoclonal antibody (94) to the human IgG_1 C_H3 domain. The diabodies, expressed in NS0 mouse myeloma cells, bound to the human HER-2 overexpressing breast cancer cell line, MCF7/HER-2. However, the tumor uptake of directly radioiodinated 10H8 hinge-minibody in MCF7/HER-2 xenografts was much lower (max 5.6% ID/g at 12 h) in comparison to that observed with the anti-CEA minibody (max 21.4% ID/g at 12 h) (86, 95). The 10H8 minibody (80 kDa) has been labeled with ^{111}In after conjugated to DOTA. The tumor uptake of ^{111}In-DOTA 10H8 minibody was similar to that seen in the radioiodinated 10H8 minibody. The kidneys had unexpectedly high activity due to the presence of cross-reactive antigen in the kidneys. Tumor uptake of another minibody hu4D5v8 derived from trastuzumab, evaluated by quantitative microPET using ^{64}Cu-labeled minibody, also showed similarly low tumor uptake and high kidney accumulation. A larger hu4D5v8 fragment [$(scFv\text{-}C_H2\text{-}C_H3)_2$; 105 kDa] , when evaluated by microPET, exhibited improved tumor targeting efficacy and reduced kidney uptake (96). Thus, by manipulating the size and format of anti-HER-2 antibody fragments, the kidney activity can be reduced.

3.5. Affibodies

Affibody molecules are small non-immunoglobulin affinity ligands based on a 58-amino-acid Z-domain scaffold, derived from one of the IgG-binding domains of *staphylococcal* protein A (97). Randomization of 13 amino acid positions in the binding surface of this domain scaffold has been used to construct combinatorial phagemid libraries, from which affibody molecules bound to desired target molecules can be selected by phage display (98, 99). The affibody molecule $His_6\text{-}Z_{HER\text{-}2/neu:4}$ was demonstrated to bind with nanomolar affinity (approximately 50 nM) to the HER-2-ECD molecule at a different site than the humanized antibody trastuzumab. ^{125}I labeled $His_6\text{-}Z_{HER\text{-}2/neu:4}$ affibody made by indirect radioiodination using N-succinimidyl-p-(trimethylstannyl) benzoate (SPMB) showed specific binding to native HER-2 overexpressed on the SKBR-3 tumor cell line (100, 101). The bivalent form of the affibody ligand, $(Z_{HER\text{-}2:4})_2$ has a molecular weight of 15.6 kDa and an apparent affinity (K_D) against HER-2 of 3 nM, which is approximately the same as trastuzumab. After radioiodination with the linker molecule SPMB, *in vitro* binding assays showed specific binding to HER-2 overexpressing SKOV-3 cells. Internalization of ^{125}I was shown after delivery with both the monovalent and the bivalent affibodies. The cellular retention of ^{125}I was longer after delivery with the bivalent affibody compared with the monovalent affibody (102). Due to its small size, ^{125}I- $(Z_{HER\text{-}2:4})_2$ affibody was primarily excreted through the kidneys, which caused extremely high kidney accumulation. Significant amounts of radioactivity were specifically targeted to SKOV-3 tumors as evidenced by the biodistribution study. A tumor-to-blood ratio of about 10:1 was obtained at 8 h post injection, and the tumors could be easily visualized with a gamma camera at this time point (103). The second-generation HER-2-specific affibody molecule ($His_6\text{-}Z_{HER\text{-}2:342}$), obtained by a single-library affinity maturation, bound HER-2 with a K_D of 22 pM. Gamma camera imaging with ^{125}I-SPMB- $His_6\text{-}Z_{HER\text{-}2:342}$ showed clear, high-contrast visualization of HER-

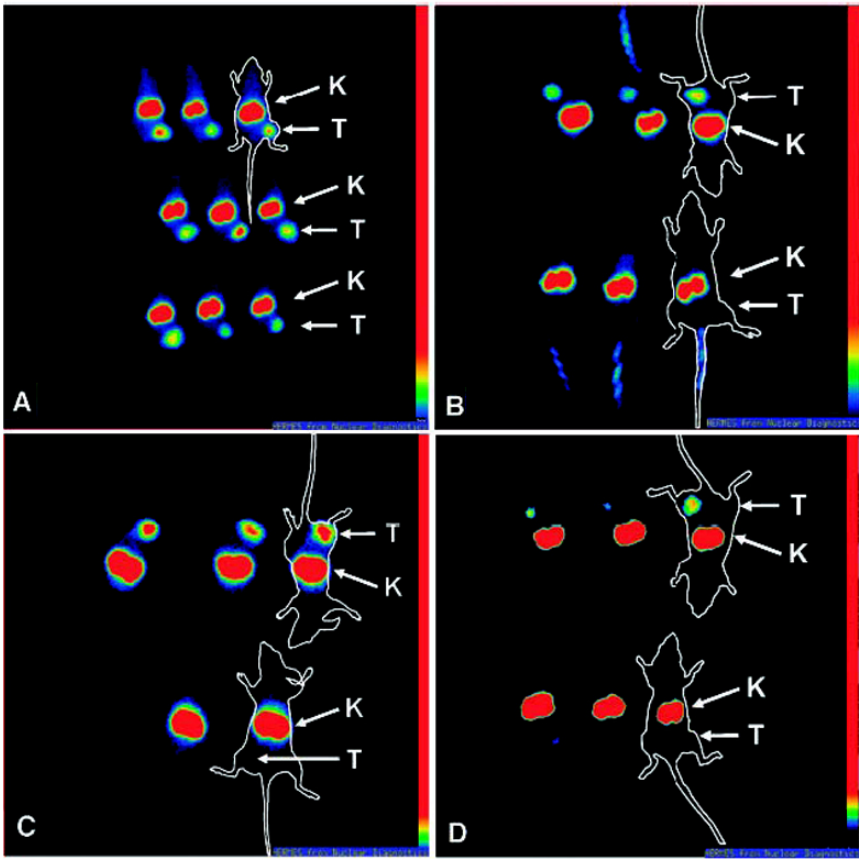

Figure 7. Gamma camera images of HER-2-expressing SKOV-3 xenograft tumors in BALB/c nu/nu mice. (A) Imaging of mice at different time points after injection, 1 h (top), 2 h (middle), and 4 h (bottom) after injection of ^{111}In-DOTA-$Z_{HER-2:342-pep2}$. (B) Imaging of mice pre-blocked (bottom) or not blocked (top) with 0.9 mg of unlabeled $Z_{HER-2:342}$ 45 min before injection of ^{111}In-DOTA-$Z_{HER-2:342-pep2}$. Imaging was done 1 h after injection. (C) Imaging of mice injected with ^{111}In-DOTA-$Z_{HER-2:342-pep2}$ (top) or ^{111}In-DOTA-$Z_{taq4:5}$ (bottom) 4 h after injection. (D) Imaging of mice 4 h after injection, pretreated with 17-AAG (bottom) and controls (top). Adapted with permission from ref. 107.

2-expressing xenografts in mice as early as 6 hours post-injection. Due to increased affinity, the uptake for $Z_{HER2:342}$, compared to the parental $Z_{HER2:4}$ monomer, improved by 2.03, 3.94, and 24.29 times at 1, 4, and 24 hours, respectively, with a tumor uptake of ~ 9% ID/g at 4 hours. (104). ^{111}In is one of the most commonly used radionuclide for single-photon imaging with good imaging properties, facile logistics of delivery, and well studied labeling chemistry. Conjugation of isothiocyanate-benzyl-DTPA to $Z_{HER-2:342}$ has been performed using a chelator-to-protein molar ratio of 1:1. The affinity of ^{111}In-labeled $Z_{HER-2:342}$ to HER-2 was 21 pM, according to surface plasmon resonance (SPR) measurements. HER-2-expressing SKOV-3 xenografts in nude mice were clearly imaged 4 h after injection by using a gamma-camera (105).

Radiolabeling chemistries relying on amine or thiol-reactive reagents usually result in a heterogeneous mixture of tracers with different numbers of chelators owing to multiple reactive groups in the peptides and proteins. The relatively small size of affibody molecules enables a direct chemical peptide synthesis at high yields (106). By using synthetic chemistry, the chelator can be introduced site specifically, thus generating a homogeneous tracer with well-defined properties. The affibody molecule $Z_{HER-2:342-pep2}$, site-specifically and homogeneously conjugated with a DOTA chelator, has been produced in a single chemical process by standard Fmoc solid phase peptide synthesis. DOTA-$Z_{HER-2:342-pep2}$ bound HER-2 with 65 pmol/L affinity. High-contrast gamma camera images showed high tumor uptake at 1 h after injection of ^{111}In-DOTA-$Z_{HER-2:342-pep2}$. Pretreatment with trastuzumab did not interfere with tumor targeting, which could be due to a different binding site of trastuzumab and the affibody with HER-2. Degradation of HER-2 using the heat shock protein 90 inhibitor 17-AAG before administration of ^{111}In-DOTA-$Z_{HER-2:342-pep2}$ obliterated the tumor uptake. This indicates that the affibody might be useful in monitoring tumor response to HER-2 targeted therapy, including Hsp90 inhibitors (Figure 7) (107). Similar to other affibody molecules, extremely high ^{111}In-DOTA-$Z_{HER-2:342-pep2}$ accumulation in kidneys has been observed. The small molecule size of the affibody might partially account for this phenomenon. However, the presence of cross-reactive antigen in kidneys cannot be excluded (108).

Histidine tag, MAG3 chelator and the natural peptide sequences cysteine-diglycine (CGG) and cysteine-triglycine (CGGG) sequences have been incorporated into $Z_{HER-2:342}$ by using peptide synthesis for site specific labeling of ^{99m}Tc (109-111). After labeling with ^{99m}Tc, all affibody molecules demonstrated tumor-specific uptake, which could be visualized by gamma camera imaging at 6 h after injection. Compared with MAG3 chelator, ^{99m}Tc-labeled cysteine-based chelators seemed to exhibit comparable tumor-to-organ ratios as the other ^{99m}Tc - labeled affibodies, if not better. It also showed a 3-fold reduction of hepatobiliary excretion (111). The use of cysteine instead of mercaptoacetyl as a thiol group donor increased the overall hydrophilicity of the chelate due to the presence of a charged amino group and a shift in the excretion pathway from hepatobiliary to renal, which resulted in higher kidney accumulation (112). Moreover, elevated radioactivity in the stomach and salivary glands was observed with ^{99m}Tc-CGGG-$Z_{HER-2:342}$, indicating some release of free pertechnetate. It is likely that the release occurred during the catabolism of the labeled conjugates in kidney and reoxidation (111).

4. SUMMARY AND PERSPECTIVE

With HER-2 specific antibodies, antibody derivatives and affibodies, numerous studies have been performed to image HER-2 expression with such diverse imaging modalities as optical imaging, MRI, and radionuclide imaging (gamma camera, SPECT and PET). To date, however, most studies have been proof-of-principle experiments that sought to demonstrate the feasibility to visualize *in vivo* HER-2 overexpression. The uptake values of each tracer at one or several time points post injection needed to be quantified by *ex vivo* biodistribution measurement (79, 88, 113). To better evaluate HER-2 expression non-invasively, the challenges such as the selection of antibody ligand and radioisotope, bioconjugation and immunoreactivity, metabolic stability, and *in vivo* kinetics of the imaging tracers all need to be optimized.

Due to their smaller size, antibody fragments, scFv, and affibodies are superior in blood clearance and tumor penetration. This enables repetitive imaging at short time intervals. However, in cases such as confirmation of tumor targeting and estimation of radiation dose delivery to both tumor and normal tissues for RIT, intact antibodies are irreplaceable. RII with intact antibodies can be used for *in vivo* characterization of new RIT candidate mAbs, as well as for the selection of RIT candidate patients, which is routine in both the Zevalin and Bexxar treatment regimens (114, 115). A similar strategy could be used in HER-2 targeted RIT with therapeutic radioisotope labeled trastuzumab. The radiation burden to the patient caused by PET imaging due to long biologic half-lives of intact Abs (116) could be mitigated by the introduction of PET scanners with higher sensitivity, allowing comparable images to be acquired with lower doses of injected radioactivity.

Radionuclide selection and labeling is another important issue for successful imaging. The ideal radionuclide for PET imaging would have suitable half-lives, *i.e.* a long half-life for intact Ab and a shorter one for Ab fragment, scFv or small molecules. High β^+ particle energy will cause intrinsic resolution loss (^{68}Ga, ^{76}Br, and ^{124}I) and the presence of prompt single-photons will lead to spurious true coincidences (^{86}Y ($t_{1/2}$ = 14.7 h), ^{76}Br ($t_{1/2}$ = 16.2 h)). Presence of radionuclidic impurities or radioisotopes of the same element generated during cyclotron production (e.g. ^{64}Cu) will also cause problem for labeling and quantification (116). It would be helpful to use imaging figure of merit (IFOM) criterion to determine which radionuclide is best suited as a radiolabel for the selected antibody or affibody molecule (117).

The stability of radiolabeled conjugates is another critical component for imaging quantification. Direct iodination of antibodies often suffers from dehalogenation via deiodinases, enzymes that may not distinguish radioiodinated tyrosines from thyroxine (118). To circumvent this problem, HER-2 specific antibodies and affibodies have been indirectly iodinated by introducing acylating agents such as PIB and SMPB (38, 55, 104). The labeling of metal radioisotopes such as ^{99m}Tc, ^{111}In and ^{64}Cu are usually done through chelator conjugation to antibodies. After internalization and proteolytic degradation of targeting protein by tumor cells, these isotopes including ^{64}Cu and ^{111}In will be trapped intracellularly (119, 120). By improving tumor accumulation, this process may enable better visualization. On the other hand, it will also likely cause overestimation of HER-2 expression.

For clinical application, site-specific, homogenous, reproducible, and easy radiolabeling is desirable. However, the most commonly used targeting agents are usually modified at multiple and randomly distributed sites by using modification chemistries based on amine, thiol or tyrosine-reactive reagents. Thus, the resulting targeting molecules are heterogeneous with various degrees of modification. By using synthetic chemistry of HER-2 specific affibody molecules, the chelators can be introduced site specifically (107, 109-111). Site specific radiolabeling and imaging for relatively small biomolecules such as VEGF (121), scFv (122) have been reported. The optimal strategies for intact antibody site specific labeling, however, remain to be worked out. ROI analysis techniques currently used for imaging quantification need to outline the tumor region on images. The continuing development of PET/CT and PET/MRI will provide more accurate tumor outlining based on the anatomical images acquired by CT or MRI (123).

HER-2 expression monitoring is not only crucial to HER-2 directly targeting immunotherapy or RIT, but also is important in other related chemotherapies. For example, HER-2 is one of the critical client proteins for Hsp90, and HER-2 level inside tumors declines dramatically upon heat shock protein 90 inhibitor, 17-AAG treatment. HER-2 degradation during 17-AAG treatment could be visualized and quantified by ^{68}Ga-HER-2-PET (77). More importantly, HER-2 PET is an earlier predictor of tumor response to 17-AAG therapy than ^{18}F-FDG PET

(78). Histone deacetylase (HDAC) is capable of regulating gene expression through diverse mechanisms, including modulation of the histone code and acetylation of many non–histone proteins (124, 125). HDAC inhibitors are a structurally diverse group of drugs that show preclinical and clinical promise as cancer therapeutics (126). HDAC inhibitors, for instance, can selectively reduce HER-2 expression by repressing the HER-2 promoter and accelerating the decay of cytoplasmic HER-2 transcripts (20). HER-2 imaging might be also valuable in predicting early response of HDAC inhibitors therapy.

In summary, molecular imaging with multiple modalities has made impressive progress in monitoring HER-2 expression. With the continuing development of both imaging tracers and facilities, HER-2 imaging will likely prove valuable in lesion detection, patient stratification, and treatment monitoring.

5. ACKNOWLEDGMENT

This project was supported by National Institute of Biomedical Imaging and Bioengineering (NIBIB) (R21 EB001785), National Cancer Institute (NCI) (R21 CA102123, P50 CA114747, U54 CA119367, and R24 CA93862), Department of Defense (DOD) (W81XWH-04-1-0697, W81XWH-06-1-0665, W81XWH-06-1-0042, and DAMD17-03-1-0143), and a Benedict Cassen Postdoctoral Fellowship from the Education and Research Foundation of the Society of Nuclear Medicine (to W. Cai).

6. REFERENCES

1. A. L. Schechter, M. C. Hung, L. Vaidyanathan, R. A. Weinberg, T. L. Yang-Feng, U. Francke, A. Ullrich and L. Coussens: The neu gene: an erbB-homologous gene distinct from and unlinked to the gene encoding the EGF receptor. *Science* 229(4717), 976-978 (1985)

2. F. Meric-Bernstam and M.-C. Hung: Advances in targeting human epidermal growth factor receptor-2 signaling for cancer therapy. *Clin Cancer Res* 12(21), 6326-6330 (2006)

3. C. I. Bargmann, M. C. Hung and R. A. Weinberg: Multiple independent activations of the neu oncogene by a point mutation altering the transmembrane domain of p185. *Cell* 45(5), 649-657. (1986)

4. M. Tan, J. Yao and D. Yu: Overexpression of the c-erbB-2 gene enhanced intrinsic metastasis potential in human breast cancer cells without increasing their transformation abilities. *Cancer Res* 57(6), 1199-1205. (1997)

5. S. S. Bacus, S. G. Ruby, D. S. Weinberg, D. Chin, R. Ortiz and J. W. Bacus: HER-2/neu oncogene expression and proliferation in breast cancers. *Am J Pathol* 137(1), 103-111 (1990)

6. A. M. Traish and H. H. Wotiz: Prostatic epidermal growth factor receptors and their regulation by androgens. *Endocrinology* 121(4), 1461-1467 (1987)

7. A. Hofer, J. C. Saez, C. C. Chang, J. E. Trosko, D. C. Spray and R. Dermietzel: C-erbB2/neu transfection induces gap junctional communication incompetence in glial cells. *J Neurosci* 16(14), 4311-4321 (1996)

8. D. J. Slamon, W. Godolphin, L. A. Jones, J. A. Holt, S. G. Wong, D. E. Keith, W. J. Levin, S. G. Stuart, J. Udove, A. Ullrich and *et al.*: Studies of the HER-2/neu proto-oncogene in human breast and ovarian cancer. *Science* 244(4905), 707-712. (1989)

9. P. M. Schneider, M. C. Hung, S. M. Chiocca, J. Manning, X. Y. Zhao, K. Fang and J. A. Roth: Differential expression of the c-erbB-2 gene in human small cell and non-small cell lung cancer. *Cancer Res* 49(18), 4968-4971. (1989)

10. U. Fischer, L. Kopka, U. Brinck, M. Korabiowska, A. Schauer and E. Grabbe: Prognostic value of contrast-enhanced MR mammography in patients with breast cancer. *Eur Radiol* 7(7), 1002-1005 (1997)

11. J. W. Park, R. Stagg, G. D. Lewis, P. Carter, D. Maneval, D. J. Slamon, H. Jaffe and H. M. Shepard: Anti-p185HER2 monoclonal antibodies: biological properties and potential for immunotherapy. *Cancer Treat Res* 61, 193-211 (1992)

12. C. D. Austin, A. M. De Maziere, P. I. Pisacane, S. M. van Dijk, C. Eigenbrot, M. X. Sliwkowski, J. Klumperman and R. H. Scheller: Endocytosis and sorting of ErbB2 and the site of action of cancer therapeutics trastuzumab and geldanamycin. *Mol Biol Cell* 15(12), 5268-5282 (2004)

13. M. Pegram, S. Hsu, G. Lewis, R. Pietras, M. Beryt, M. Sliwkowski, D. Coombs, D. Baly, F. Kabbinavar and D. Slamon: Inhibitory effects of combinations of HER-2/neu antibody and chemotherapeutic agents used for treatment of human breast cancers. *Oncogene* 18(13), 2241-2251. (1999)

14. M. S. Tai, J. E. McCartney, G. P. Adams, D. Jin, R. M. Hudziak, H. Oppermann, A. A. Laminet, M. A. Bookman, E. J. Wolf, S. Liu and *et al.*: Targeting c-erbB-2 expressing tumors using single-chain Fv monomers and dimers. *Cancer Res* 55(23 Suppl), 5983s-5989s (1995)

15. J. Baselga, D. Tripathy, J. Mendelsohn, S. Baughman, C. C. Benz, L. Dantis, N. T. Sklarin, A. D. Seidman, C. A. Hudis, J. Moore, P. P. Rosen, T. Twaddell, I. C. Henderson and L. Norton: Phase II study of weekly intravenous trastuzumab (Herceptin) in patients with HER2/neu-overexpressing metastatic breast cancer. *Semin Oncol* 26(4 Suppl 12), 78-83. (1999)

16. D. B. Agus, R. W. Akita, W. D. Fox, G. D. Lewis, B. Higgins, P. I. Pisacane, J. A. Lofgren, C. Tindell, D. P. Evans, K. Maiese, H. I. Scher and M. X. Sliwkowski: Targeting ligand-activated ErbB2 signaling inhibits breast and prostate tumor growth. *Cancer Cell* 2(2), 127-137 (2002)

17. R. Nahta, M. C. Hung and F. J. Esteva: The HER-2-targeting antibodies trastuzumab and pertuzumab synergistically inhibit the survival of breast cancer cells. *Cancer Res* 64(7), 2343-2346 (2004)

18. G. E. Konecny, M. D. Pegram, N. Venkatesan, R. Finn, G. Yang, M. Rahmeh, M. Untch, D. W. Rusnak, G. Spehar, R. J. Mullin, B. R. Keith, T. M. Gilmer, M. Berger, K. C. Podratz and D. J. Slamon: Activity of the dual kinase inhibitor lapatinib (GW572016) against HER-2-overexpressing and trastuzumab-treated breast cancer cells. *Cancer Res* 66(3), 1630-1639. (2006)

19. D. B. Solit, F. F. Zheng, M. Drobnjak, P. N. Münster, B. Higgins, D. Verbel, G. Heller, W. Tong, C. Cordon-Cardo, D. B. Agus, H. I. Scher and N. Rosen: 17-

Allylamino-17-demethoxygeldanamycin induces the degradation of androgen receptor and HER-2/neu and inhibits the growth of prostate cancer xenografts. *Clin Cancer Res* 8(5), 986-993 (2002)
20. D. C. Drummond, C. Marx, Z. Guo, G. Scott, C. Noble, D. Wang, M. Pallavicini, D. B. Kirpotin and C. C. Benz: Enhanced Pharmacodynamic and Antitumor Properties of a Histone Deacetylase Inhibitor Encapsulated in Liposomes or ErbB2-Targeted Immunoliposomes. *Clin Cancer Res* 11(9), 3392-3401 (2005)
21. A. Thybusch-Bernhardt, A. Aigner, S. Beckmann, F. Czubayko and H. Juhl: Ribozyme targeting of HER-2 inhibits pancreatic cancer cell growth *in vivo*. *Eur J Cancer* 37(13), 1688-1694 (2001)
22. W. B. Tan, S. Jiang and Y. Zhang: Quantum-dot based nanoparticles for targeted silencing of HER2/neu gene via RNA interference. *Biomaterials* 28(8), 1565-1571 (2007)
23. S. Menard, P. Casalini, M. Campiglio, S. M. Pupa and E. Tagliabue: Role of HER2/neu in tumor progression and therapy. *Cell Mol Life Sci* 61(23), 2965-2978 (2004)
24. R. C. Bast, P. Ravdin, D. F. Hayes, S. Bates, H. Fritsche, J. M. Jessup, N. Kemeny, G. Y. Locker, R. G. Mennel and M. R. Somerfield: 2000 update of recommendations for the use of tumor markers in breast and colorectal cancer: clinical practice guidelines of the American Society of Clinical Oncology. *J Clin Oncol* 19(6), 1865-1878 (2001)
25. D. T. McManus, A. H. Patterson, P. Maxwell, M. W. Humphreys and N. H. Anderson: Fluorescence *in situ* hybridisation detection of erbB2 amplification in breast cancer fine needle aspirates. *Mol Pathol* 52(2), 75-77 (1999)
26. P. C. Stomper, R. M. Budnick and C. C. Stewart: Use of specimen mammography-guided FNA (fine-needle aspirates) for flow cytometric multiple marker analysis and immunophenotyping in breast cancer. *Cytometry* 42(3), 165-173 (2000)
27. T. F. Massoud and S. S. Gambhir: Molecular imaging in living subjects: seeing fundamental biological processes in a new light. *Genes Dev* 17(5), 545-580 (2003)
28. J. H. Thrall: Personalized Medicine. *Radiology* 231(3), 613-616 (2004)
29. P. Holliger and P. J. Hudson: Engineered antibody fragments and the rise of single domains. *Nat Biotech* 23(9), 1126-1136 (2005)
30. R. W. Baldwin and M. V. Pimm: Antitumor monoclonal antibodies for radioimmunodetection of tumors and drug targeting. *Cancer Metastasis Rev* 2(1), 89-106 (1983)
31. D. M. Goldenberg: Current status of cancer imaging with radiolabeled antibodies. *J Cancer Res Clin Oncol* 113(3), 203-208 (1987)
32. T. Saga, K. Endo, T. Akiyama, H. Sakahara, M. Koizumi, Y. Watanabe, T. Nakai, M. Hosono, T. Yamamoto, K. Toyoshima and *et al.*: Scintigraphic detection of overexpressed c-erbB-2 protooncogene products by a class-switched murine anti-c-erbB-2 protein monoclonal antibody. *Cancer Res* 51(3), 990-994 (1991)
33. J. M. Styles, S. Harrison, B. A. Gusterson and C. J. Dean: Rat monoclonal antibodies to the external domain of the product of the C-erbB-2 proto-oncogene. *Int J Cancer* 45(2), 320-324 (1990)
34. C. J. Dean, S. A. Eccles, M. Valeri, G. Box, S. Allan, C. McFarlane, J. Sandle and J. Styles: Rat MAbs to the product of the c-erbB-2 proto-oncogene for diagnosis and therapy in breast cancer. *Cell Biophys* 22(1-3), 111-127 (1993)
35. W. J. Smellie, C. J. Dean, N. P. Sacks, M. R. Zalutsky, P. K. Garg, P. Carnochan and S. A. Eccles: Radioimmunotherapy of breast cancer xenografts with monoclonal antibody ICR12 against c-erbB2 p185: comparison of iodogen and N-succinimidyl 4-methyl-3-(tri-n-butylstannyl)benzoate radioiodination methods. *Cancer Res* 55(23 Suppl), 5842s-5846s (1995)
36. S. M. Allan, C. J. Dean, S. Eccles and N. P. Sacks: Clinical radioimmunolocalization with a rat monoclonal antibody directed against c-erbB-2. *Cell Biophys* 24-25, 93-98 (1994)
37. A. Meenakshi, R. S. Kumar, V. Ganesh and N. S. Kumar: Preliminary study on radioimmunodiagnosis of experimental tumor models using technetium-99m-labeled anti-C-erbB-2 monoclonal antibody. *Tumori* 88(6), 507-512 (2002)
38. M. A. Bakir, S. Eccles, J. W. Babich, N. Aftab, J. Styles, C. J. Dean, R. M. Lambrecht and R. J. Ott: c-erbB2 protein overexpression in breast cancer as a target for PET using iodine-124-labeled monoclonal antibodies. *J Nucl Med* 33(12), 2154-2160 (1992)
39. S. Göhr-Rosenthal, H. Schmitt-Willich, W. Ebert and J. Conrad: The demonstration of human tumors on nude mice using gadolinium-labelled monoclonal antibodies for magnetic resonance imaging. *Invest Radiol* 28(9), 789-795 (1993)
40. R. M. Sharkey, T. M. Cardillo, E. A. Rossi, C.-H. Chang, H. Karacay, W. J. McBride, H. J. Hansen, I. D. Horak and D. M. Goldenberg: Signal amplification in molecular imaging by pretargeting a multivalent, bispecific antibody. *Nature Med* 11(11), 1250-1255 (2005)
41. D. Artemov, N. Mori, R. Ravi and Z. M. Bhujwalla: Magnetic resonance molecular imaging of the HER-2/neu receptor. *Cancer Res* 63(11), 2723-2727 (2003)
42. M. A. Funovics, B. Kapeller, C. Hoeller, H. S. Su, R. Kunstfeld, S. Puig and K. Macfelda: MR imaging of the her2/neu and 9.2.27 tumor antigens using immunospecific contrast agents. *Magn Reson Imaging* 22(6), 843-850 (2004)
43. J. S. Sandhu: Protein engineering of antibodies. *Crit Rev Biotechnol* 12(5-6), 437-462 (1992)
44. H. M. Shepard, G. D. Lewis, J. C. Sarup, B. M. Fendly, D. Maneval, J. Mordenti, I. Figari, C. E. Kotts, M. A. Palladino, Jr., A. Ullrich and *et al.*: Monoclonal antibody therapy of human cancer: taking the HER2 protooncogene to the clinic. *J Clin Immunol* 11(3), 117-127 (1991)
45. P. Carter, L. Presta, C. M. Gorman, J. B. Ridgway, D. Henner, W. L. Wong, A. M. Rowland, C. Kotts, M. E. Carver and H. M. Shepard: Humanization of an anti-p185HER2 antibody for human cancer therapy. *Proc Natl Acad Sci U S A* 89(10), 4285-4289 (1992)
46. C. E. Kotts, F. M. Su, C. Leddy, T. Dodd, S. Scates, M. R. Shalaby, C. M. Wirth, D. Giltinan, R. W. Schroff, A. R. Fritzberg, H. M. Shepard, D. J. Slamon and B. M. Hutchins: ^{186}Re-labeled antibodies to p185HER2 as HER2-targeted radioimmunopharmaceutical agents: comparison of physical and biological characteristics with ^{125}I and ^{131}I-

labeled counterparts. *Cancer Biother Radiopharm* 11(2), 133-144 (1996)
47. R. Wiercioch, E. Balcerczak, E. Byszewska and M. Mirowski: Uptake of radiolabelled herceptin by experimental mammary adenocarcinoma. *Nucl Med Rev Cent East Eur* 6(2), 99-103 (2003)
48. M. Persson, V. Tolmachev, K. Andersson, L. Gedda, M. Sandstrom and J. Carlsson: [^{177}Lu]pertuzumab: experimental studies on targeting of HER-2 positive tumour cells. *Eur J Nucl Med Mol Imaging* 32(12), 1457-1462 (2005)
49. M. N. Lub-de Hooge, J. G. Kosterink, P. J. Perik, H. Nijnuis, L. Tran, J. Bart, A. J. Suurmeijer, S. de Jong, P. L. Jager and E. G. de Vries: Preclinical characterisation of ^{111}In-DTPA-trastuzumab. *Br J Pharmacol* 143(1), 99-106 (2004)
50. P. J. Perik, M. N. Lub-De Hooge, J. A. Gietema, W. T. van der Graaf, M. A. de Korte, S. Jonkman, J. G. Kosterink, D. J. van Veldhuisen, D. T. Sleijfer, P. L. Jager and E. G. de Vries: Indium-111-labeled trastuzumab scintigraphy in patients with human epidermal growth factor receptor 2-positive metastatic breast cancer. *J Clin Oncol* 24(15), 2276-2282 (2006)
51. C. Waldherr, M. Pless, H. R. Maecke, A. Haldemann and J. Mueller-Brand: The clinical value of [^{90}Y-DOTA]-D-Phe1-Tyr3-octreotide (^{90}Y-DOTATOC) in the treatment of neuroendocrine tumours: a clinical phase II study. *Ann Oncol* 12(7), 941-945 (2001)
52. K. Garmestani, D. E. Milenic, P. S. Plascjak and M. W. Brechbiel: A new and convenient method for purification of ^{86}Y using a Sr(II) selective resin and comparison of biodistribution of ^{86}Y and ^{111}In labeled Herceptin. *Nucl Med Biol* 29(5), 599-606 (2002)
53. A. Lövqvist, J. L. Humm, A. Sheikh, R. D. Finn, J. Koziorowski, S. Ruan, K. S. Pentlow, A. Jungbluth, S. Welt, F. T. Lee, M. W. Brechbiel and S. M. Larson: PET imaging of ^{86}Y-labeled anti-Lewis Y monoclonal antibodies in a nude mouse model: comparison between ^{86}Y and ^{111}In radiolabels. *J Nucl Med* 42(8), 1281-1287 (2001)
54. S. Palm, R. M. Enmon, Jr., C. Matei, K. S. Kolbert, S. Xu, P. B. Zanzonico, R. L. Finn, J. A. Koutcher, S. M. Larson and G. Sgouros: Pharmacokinetics and Biodistribution of ^{86}Y-Trastuzumab for ^{90}Y dosimetry in an ovarian carcinoma model: correlative MicroPET and MRI. *J Nucl Med* 44(7), 1148-1155 (2003)
55. A. Bruskin, I. Sivaev, M. Persson, H. Lundqvist, J. Carlsson, S. Sjoberg and V. Tolmachev: Radiobromination of monoclonal antibody using potassium [^{76}Br] (4 isothiocyanatobenzyl-ammonio)-bromo-decahydro-closo-dodecaborate (Bromo-DABI). *Nucl Med Biol* 31(2), 205-211 (2004)
56. E. Mume, A. Orlova, P. U. Malmstrom, H. Lundqvist, S. Sjoberg and V. Tolmachev: Radiobromination of humanized anti-HER2 monoclonal antibody trastuzumab using N-succinimidyl 5-bromo-3-pyridinecarboxylate, a potential label for immunoPET. *Nucl Med Biol* 32(6), 613-622 (2005)
57. S. J. Dodd, M. Williams, J. P. Suhan, D. S. Williams, A. P. Koretsky and C. Ho: Detection of single mammalian cells by high-resolution magnetic resonance imaging. *Biophys J* 76(1 Pt 1), 103-109 (1999)
58. D. Artemov, N. Mori, B. Okollie and Z. M. Bhujwalla: MR molecular imaging of the Her-2/neu receptor in breast cancer cells using targeted iron oxide nanoparticles. *Magn Reson Med* 49(3), 403-408 (2003)
59. J. H. Lee, Y. M. Huh, Y. W. Jun, J. W. Seo, J. T. Jang, H. T. Song, S. Kim, E. J. Cho, H. G. Yoon, J. S. Suh and J. Cheon: Artificially engineered magnetic nanoparticles for ultra-sensitive molecular imaging. *Nat Med* 13(1), 95-99 (2007)
60. J. W. M. Bulte and D. L. Kraitchman: Iron oxide MR contrast agents for molecular and cellular imaging. *NMR in Biomedicine* 17(7), 484-499 (2004)
61. H. B. Na, J. H. Lee, K. An, Y. I. Park, M. Park, I. S. Lee, D. Nam, S. T. Kim, S. Kim, S. K. Kim, K. H. Lim, K. S. Kim, S. O. Kim and T. Hyeon: Development of a T_1 contrast agent for magnetic resonance imaging using MnO nanoparticles. *Angewandte Chemie (International ed)* (2007)
62. V. Ntziachristos and B. Chance: Accuracy limits in the determination of absolute optical properties using time-resolved NIR spectroscopy. *Med Phy* 28(6), 1115-1124 (2001)
63. I. Hilger, Y. Leistner, A. Berndt, C. Fritsche, K. M. Haas, H. Kosmehl and W. A. Kaiser: Near-infrared fluorescence imaging of HER-2 protein over-expression in tumour cells. *Eur Radiol* 14(6), 1124-1129 (2004)
64. M. Bruchez, M. Moronne, P. Gin, S. Weiss and A. P. Alivisatos: Semiconductor nanocrystals as fluorescent biological labels. *Science* 281(5385), 2013-2016 (1998)
65. X. Wu, H. Liu, J. Liu, K. N. Haley, J. A. Treadway, J. P. Larson, N. Ge, F. Peale and M. P. Bruchez: Immunofluorescent labeling of cancer marker Her2 and other cellular targets with semiconductor quantum dots. *Nat Biotechnol* 21(1), 41-46 (2003)
66. C. Loo, L. Hirsch, M. H. Lee, E. Chang, J. West, N. Halas and R. Drezek: Gold nanoshell bioconjugates for molecular imaging in living cells. *Opt Lett* 30(9), 1012-1014 (2005)
67. C. Loo, A. Lowery, N. Halas, J. West and R. Drezek: Immunotargeted nanoshells for integrated cancer imaging and therapy. *Nano Lett* 5(4), 709-711 (2005)
68. J. M. Esteban, D. Colcher, P. Sugarbaker, J. A. Carrasquillo, G. Bryant, A. Thor, J. C. Reynolds, S. M. Larson and J. Schlom: Quantitative and qualitative aspects of radiolocalization in colon cancer patients of intravenously administered MAb B72.3. *Int J Cancer* 39(1), 50-59 (1987)
69. M. A. Clauss and R. K. Jain: Interstitial transport of rabbit and sheep antibodies in normal and neoplastic tissues. *Cancer Res* 50(12), 3487-3492 (1990)
70. A. M. Wu and P. D. Senter: Arming antibodies: prospects and challenges for immunoconjugates. *Nature Biotechnol* 23(9), 1137-1146 (2005)
71. M. Jain and S. K. Batra: Genetically engineered antibody fragments and PET imaging: A new era of radioimmunodiagnosis. *J Nucl Med* 44(12), 1970-1972 (2003)
72. Y. Tang, D. Scollard, P. Chen, J. Wang, C. Holloway and R. M. Reilly: Imaging of HER2/neu expression in BT-474 human breast cancer xenografts in athymic mice using [^{99m}Tc]-HYNIC-trastuzumab (Herceptin) Fab fragments. *Nucl Med Commun* 26(5), 427-432 (2005)

73. Y. Tang, J. Wang, D. A. Scollard, H. Mondal, C. Holloway, H. J. Kahn and R. M. Reilly: Imaging of HER2/neu-positive BT-474 human breast cancer xenografts in athymic mice using ^{111}In-trastuzumab (Herceptin) Fab fragments. *Nucl Med Biol* 32(1), 51-58 (2005)
74. M. S. Dennis, H. Jin, D. Dugger, R. Yang, L. McFarland, A. Ogasawara, S. Williams, M. J. Cole, S. Ross and R. Schwall: Imaging tumors with an albumin-binding Fab, a novel tumor-targeting agent. *Cancer Res* 67(1), 254-261 (2007)
75. A. Nguyen, A. E. Reyes, II, M. Zhang, P. McDonald, W. L. T. Wong, L. A. Damico and M. S. Dennis: The pharmacokinetics of an albumin-binding Fab (AB.Fab) can be modulated as a function of affinity for albumin. *Protein Eng Des Sel* 19(7), 291-297 (2006)
76. E. Tokunaga, E. Oki, K. Nishida, T. Koga, A. Egashira, M. Morita, Y. Kakeji and Y. Maehara: Trastuzumab and breast cancer: developments and current status. *Int J Clin Oncol* 11(3), 199-208 (2006)
77. P. M. Smith-Jones, D. B. Solit, T. Akhurst, F. Afroze, N. Rosen and S. M. Larson: Imaging the pharmacodynamics of HER2 degradation in response to Hsp90 inhibitors. *Nat Biotechnol* 22(6), 701-706 (2004)
78. P. M. Smith-Jones, D. Solit, F. Afroze, N. Rosen and S. M. Larson: Early tumor response to Hsp90 therapy using HER2 PET: comparison with ^{18}F-FDG PET. *J Nucl Med* 47(5), 793-796 (2006)
79. G. P. Adams, J. E. McCartney, M. S. Tai, H. Oppermann, J. S. Huston, W. F. Stafford, 3rd, M. A. Bookman, I. Fand, L. L. Houston and L. M. Weiner: Highly specific *in vivo* tumor targeting by monovalent and divalent forms of 741F8 anti-c-erbB-2 single-chain Fv. *Cancer Res* 53(17), 4026-4034 (1993)
80. S. K. Batra, M. Jain, U. A. Wittel, S. C. Chauhan and D. Colcher: Pharmacokinetics and biodistribution of genetically engineered antibodies. *Curr Opin Biotechnol* 13(6), 603-608 (2002)
81. G. P. Adams, R. Schier, K. Marshall, E. J. Wolf, A. M. McCall, J. D. Marks and L. M. Weiner: Increased affinity leads to improved selective tumor delivery of single-chain Fv antibodies. *Cancer Res* 58(3), 485-490 (1998)
82. K. Fujimori, D. G. Covell, J. E. Fletcher and J. N. Weinstein: A modeling analysis of monoclonal antibody percolation through tumors: a binding-site barrier. *J Nucl Med* 31(7), 1191-1198 (1990)
83. D. Colcher, M. F. Minelli, M. Roselli, R. Muraro, D. Simpson-Milenic and J. Schlom: Radioimmunolocalization of human carcinoma xenografts with B72.3 second generation monoclonal antibodies. *Cancer Res* 48(16), 4597-4603 (1988)
84. S. Gallinger, R. M. Reilly, J. C. Kirsh, R. D. Odze, B. J. Schmocker, K. Hay, J. Polihronis, M. T. Damani, B. Shpitz and H. S. Stern: Comparative dual label study of first and second generation antitumor-associated glycoprotein-72 monoclonal antibodies in colorectal cancer patients. *Cancer Res* 53(2), 271-278 (1993)
85. A. Todorovska, R. C. Roovers, O. Dolezal, A. A. Kortt, H. R. Hoogenboom and P. J. Hudson: Design and application of diabodies, triabodies and tetrabodies for cancer targeting. *J Immunol Methods* 248(1-2), 47-66 (2001)
86. A. M. Wu and P. J. Yazaki: Designer genes: recombinant antibody fragments for biological imaging. *Q J Nucl Med* 44(3), 268-283 (2000)
87. G. P. Adams, M. S. Tai, J. E. McCartney, J. D. Marks, W. F. Stafford, 3rd, L. L. Houston, J. S. Huston and L. M. Weiner: Avidity-mediated enhancement of *in vivo* tumor targeting by single-chain Fv dimers. *Clin Cancer Res* 12(5), 1599-1605 (2006)
88. A. Goel, J. Baranowska-Kortylewicz, S. H. Hinrichs, J. Wisecarver, G. Pavlinkova, S. Augustine, D. Colcher, B. J. Booth and S. K. Batra: ^{99m}Tc-labeled divalent and tetravalent CC49 single-chain Fv's: novel imaging agents for rapid *in vivo* localization of human colon carcinoma. *J Nucl Med* 42(10), 1519-1527 (2001)
89. D. S. Wilbur, S. W. Hadley, M. D. Hylarides, P. G. Abrams, P. A. Beaumier, A. C. Morgan, J. M. Reno and A. R. Fritzberg: Development of a stable radioiodinating reagent to label monoclonal antibodies for radiotherapy of cancer. *J Nucl Med* 30(2), 216-226 (1989)
90. G. P. Adams, J. E. McCartney, E. J. Wolf, J. Eisenberg, J. S. Huston, M. A. Bookman, P. Moldofsky, W. F. Stafford, 3rd, L. L. Houston and L. M. Weiner: Enhanced tumor specificity of 741F8-1 (sFv')2, an anti-c-erbB-2 single-chain Fv dimer, mediated by stable radioiodine conjugation. *J Nucl Med* 36(12), 2276-2281 (1995)
91. D. E. Gonzalez Trotter, R. M. Manjeshwar, M. Doss, C. Shaller, M. K. Robinson, R. Tandon, G. P. Adams and L. P. Adler: Quantitation of small-animal ^{124}I activity distributions using a clinical PET/CT scanner. *J Nucl Med* 45(7), 1237-1244 (2004)
92. M. K. Robinson, M. Doss, C. Shaller, D. Narayanan, J. D. Marks, L. P. Adler, D. E. Gonzalez Trotter and G. P. Adams: Quantitative immuno-positron emission tomography imaging of HER2-positive tumor xenografts with an iodine-124 labeled anti-HER2 diabody. *Cancer Res* 65(4), 1471-1478 (2005)
93. S. Hu, L. Shively, A. Raubitschek, M. Sherman, L. E. Williams, J. Y. Wong, J. E. Shively and A. M. Wu: Minibody: A novel engineered anti-carcinoembryonic antigen antibody fragment (single-chain Fv-CH3) which exhibits rapid, high-level targeting of xenografts. *Cancer Res* 56(13), 3055-3061 (1996)
94. J. M. Park, X. Yang, J. J. Park, O. W. Press and M. F. Press: Assessment of novel anti-p185HER-2 monoclonal antibodies for internalization-dependent therapies. *Hybridoma* 18(6), 487-495 (1999)
95. T. Olafsen, G. J. Tan, C. W. Cheung, P. J. Yazaki, J. M. Park, J. E. Shively, L. E. Williams, A. A. Raubitschek, M. F. Press and A. M. Wu: Characterization of engineered anti-p185HER-2 $(scFv\text{-}CH3)_2$ antibody fragments (minibodies) for tumor targeting. *Protein Eng Des Sel* 17(4), 315-323 (2004)
96. T. Olafsen, V. E. Kenanova, G. Sundaresan, A. L. Anderson, D. Crow, P. J. Yazaki, L. Li, M. F. Press, S. S. Gambhir, L. E. Williams, J. Y. Wong, A. A. Raubitschek, J. E. Shively and A. M. Wu: Optimizing radiolabeled engineered anti-p185HER2 antibody fragments for *in vivo* imaging. *Cancer Res* 65(13), 5907-5916 (2005)
97. B. Nilsson, T. Moks, B. Jansson, L. Abrahmsen, A. Elmblad, E. Holmgren, C. Henrichson, T. A. Jones and M. Uhlen: A synthetic IgG-binding domain based on

staphylococcal protein A. *Protein Eng Des Sel* 1(2), 107-113 (1987)
98. K. Nord, J. Nilsson, B. Nilsson, M. Uhlen and P.-A. Nygren: A combinatorial library of an {alpha}-helical bacterial receptor domain. *Protein Eng Des Sel* 8(6), 601-608 (1995)
99. K. Nord, E. Gunneriusson, J. Ringdahl, S. Ståhl, M. Uhlén and P. A. Nygren: Binding proteins selected from combinatorial libraries of an alpha-helical bacterial receptor domain. *Nature biotechnol* 15(8), 772-777 (1997)
100. M. Wikman, A. C. Steffen, E. Gunneriusson, V. Tolmachev, G. P. Adams, J. Carlsson and S. Ståhl: Selection and characterization of HER2/neu-binding affibody ligands. *Protein Eng Des Sel* 17(5), 455-462 (2004)
101. T. Tran, A. Orlova, I. Sivaev, M. Sandstrom and V. Tolmachev: Comparison of benzoate- and dodecaborate-based linkers for attachment of radioiodine to HER2-targeting Affibody ligand. *Int J Mol Med* 19(3), 485-493 (2007)
102. A. C. Steffen, M. Wikman, V. Tolmachev, G. P. Adams, F. Y. Nilsson, S. Stahl and J. Carlsson: *In vitro* characterization of a bivalent anti-HER-2 affibody with potential for radionuclide-based diagnostics. *Cancer Biother Radiopharm* 20(3), 239-248 (2005)
103. A. C. Steffen, A. Orlova, M. Wikman, F. Y. Nilsson, S. Stahl, G. P. Adams, V. Tolmachev and J. Carlsson: Affibody-mediated tumour targeting of HER-2 expressing xenografts in mice. *Eur J Nucl Med Mol Imaging* 33(6), 631-638 (2006)
104. A. Orlova, M. Magnusson, T. L. Eriksson, M. Nilsson, B. Larsson, I. Hoiden-Guthenberg, C. Widstrom, J. Carlsson, V. Tolmachev, S. Stahl and F. Y. Nilsson: Tumor imaging using a picomolar affinity HER2 binding affibody molecule. *Cancer Res* 66(8), 4339-4348 (2006)
105. V. Tolmachev, F. Y. Nilsson, C. Widstrom, K. Andersson, D. Rosik, L. Gedda, A. Wennborg and A. Orlova: ^{111}In-benzyl-DTPA-$Z_{HER2:342}$, an affibody-based conjugate for *in vivo* imaging of HER2 expression in malignant tumors. *J Nucl Med* 47(5), 846-853 (2006)
106. T. Engfeldt, B. Renberg, H. Brumer, P. A. Nygren and A. E. Karlström: Chemical synthesis of triple-labelled three-helix bundle binding proteins for specific fluorescent detection of unlabelled protein. *Chembiochem* 6(6), 1043-1050 (2005)
107. A. Orlova, V. Tolmachev, R. Pehrson, M. Lindborg, T. Tran, M. Sandstrom, F. Y. Nilsson, A. Wennborg, L. Abrahmsen and J. Feldwisch: Synthetic affibody molecules: a novel class of affinity ligands for molecular imaging of HER2-expressing malignant tumors. *Cancer Res* 67(5), 2178-2186 (2007)
108. T. M. Behr, R. M. Sharkey, G. Sgouros, R. D. Blumenthal, R. M. Dunn, K. Kolbert, G. L. Griffiths, J. A. Siegel, W. S. Becker and D. M. Goldenberg: Overcoming the nephrotoxicity of radiometal-labeled immunoconjugates: improved cancer therapy administered to a nude mouse model in relation to the internal radiation dosimetry. *Cancer* 80(12 Suppl), 2591-2610 (1997)
109. T. Engfeldt, A. Orlova, T. Tran, A. Bruskin, C. Widstrom, A. E. Karlstrom and V. Tolmachev: Imaging of HER2-expressing tumours using a synthetic Affibody molecule containing the ^{99m}Tc-chelating mercaptoacetyl-glycyl-glycyl-glycyl (MAG3) sequence. *Eur J Nucl Med Mol Imaging* (2006)
110. A. Orlova, F. Y. Nilsson, M. Wikman, C. Widstrom, S. Stahl, J. Carlsson and V. Tolmachev: Comparative *in vivo* evaluation of technetium and iodine labels on an anti-HER2 affibody for single-photon imaging of HER2 expression in tumors. *J Nucl Med* 47(3), 512-519 (2006)
111. T. Tran, T. Engfeldt, A. Orlova, C. Widstrom, A. Bruskin, V. Tolmachev and A. E. Karlstrom: *In vivo* evaluation of cysteine-based chelators for attachment of 99mTc to tumor-targeting Affibody molecules. *Bioconjug Chem* 18(2), 549-558 (2007)
112. Z. Zhu, Y. Wang, Y. Zhang, G. Liu, N. Liu, M. Rusckowski and D. J. Hnatowich: A novel and simplified route to the synthesis of N3S chelators for ^{99m}Tc labeling. *Nucl Med Biol* 28(6), 703-708 (2001)
113. G. P. Adams, C. C. Shaller, E. Dadachova, H. H. Simmons, E. M. Horak, A. Tesfaye, A. J. Klein-Szanto, J. D. Marks, M. W. Brechbiel and L. M. Weiner: A single treatment of yttrium-90-labeled CHX-A"-C6.5 diabody inhibits the growth of established human tumor xenografts in immunodeficient mice. *Cancer Res* 64(17), 6200-6206 (2004)
114. G. A. Wiseman, E. Kornmehl, B. Leigh, W. D. Erwin, D. A. Podoloff, S. Spies, R. B. Sparks, M. G. Stabin, T. Witzig and C. A. White: Radiation dosimetry results and safety correlations from ^{90}Y-ibritumomab tiuxetan radioimmunotherapy for relapsed or refractory non-Hodgkin's lymphoma: combined data from 4 clinical trials. *J Nucl Med* 44(3), 465-474 (2003)
115. R. L. Wahl: The clinical importance of dosimetry in radioimmunotherapy with tositumomab and iodine I-131 tositumomab. *Semin Oncol* 30(2 Suppl 4), 31-38 (2003)
116. I. Verel, G. W. M. Visser and G. A. van Dongen: The promise of immuno-PET in radioimmunotherapy. *J Nucl Med* 46 Suppl 1, 164S-171S (2005)
117. L. E. Williams, A. Liu, A. M. Wu, T. Odom-Maryon, A. Chai, A. A. Raubitschek and J. Y. Wong: Figures of merit (FOMs) for imaging and therapy using monoclonal antibodies. *Med Phys* 22(12), 2025-2027 (1995)
118. M. R. Zalutsky and A. S. Narula: A method for the radiohalogenation of proteins resulting in decreased thyroid uptake of radioiodine. *Int J Rad Appl Instrum [A]* 38(12), 1051-1055 (1987)
119. L. A. Bass, M. Wang, M. J. Welch and C. J. Anderson: *In vivo* transchelation of copper-64 from TETA-octreotide to superoxide dismutase in rat liver. *Bioconjug Chem* 11(4), 527-532 (2000)
120. L. B. Shih, S. R. Thorpe, G. L. Griffiths, H. Diril, G. L. Ong, H. J. Hansen, D. M. Goldenberg and M. J. Mattes: The Processing and Fate of Antibodies and Their Radiolabels Bound to the Surface of Tumor Cells *In vitro*: A Comparison of Nine Radiolabels. *J Nucl Med* 35(5), 899-908 (1994)
121. M. V. Backer, Z. Levashova, V. Patel, B. T. Jehning, K. Claffey, F. G. Blankenberg and J. M. Backer: Molecular imaging of VEGF receptors in angiogenic vasculature with single-chain VEGF-based probes. *Nature Med* 13(4), 504-509 (2007)
122. A. J. George, F. Jamar, M. S. Tai, B. T. Heelan, G. P. Adams, J. E. McCartney, L. L. Houston, L. M. Weiner, H. Oppermann and A. M. Peters: Radiometal labeling of

recombinant proteins by a genetically engineered minimal chelation site: technetium-99m coordination by single-chain Fv antibody fusion proteins through a C-terminal cysteinyl peptide. *Proc Natl Acad Sci U S A* 92(18), 8358-8362 (1995)
123**.** D. Visvikis, A. Turzo, Y. Bizais and C. Cheze-Le Rest: Technology related parameters affecting quantification in positron emission tomography imaging. *Nucl Med Commun* 25(7), 637-641 (2004)
124**.** B. D. Strahl and C. D. Allis: The language of covalent histone modifications. *Nature* 403(6765), 41-45 (2000)
125**.** B. M. Turner: Cellular memory and the histone code. *Cell* 111(3), 285-291 (2002)
126**.** D. C. Drummond, C. O. Noble, D. B. Kirpotin, Z. Guo, G. K. Scott and C. C. Benz: Clinical development of histone deacetylase inhibitors as anticancer agents. *Annu Rev Pharmacol Toxicol* 45, 495-528 (2005)

Abbreviations: HER-2: human epidermal growth factor receptor 2; TKI: tyrosine kinase inhibitor; RIT: radioimmunotherapy; ECD: extracellular domain; MION: monocrystalline iron oxide nanoparticle; CT: computed tomography; MRI: magnetic resonance imaging; CDRs: complementarity determining regions; DABI : (4-isothiocyanatobenzyl-ammonio)-undecahydro-closo-dodecaborate; 17-AAG: 17-allylaminogeldanamycin; QD: quantum dot; SPIO: superparamagnetic iron oxide; PIB: N-succinimidyl p-iodobenzoate; MEIO: magnetism-engineered iron oxide; MACS: magnetic active compensation system; SPECT: single photon emission computed tomography; PET: positron emission tomography; DOTA: 1,4,7,10-tetraazacyclododecane-1,4,7,10-tetraacetic acid; % ID/g: percentage injected dose per gram of tissue

Key Words: Human epidermal growth factor receptor 2, HER-2, Positron emission tomography, PET, Single Photon Emission Computed Tomography, SPECT, Molecular Imaging, Antibody, Affibody, Review

Send correspondence to: Xiaoyuan Chen, PhD, the Molecular Imaging Program at Stanford (MIPS), Department of Radiology and Bio-X Program, Stanford University School of Medicine, 1201 Welch Rd, P095, Stanford, CA 94305, Tel: 650-725-0950, Fax: 650-736-7925, E-mail: shawchen@stanford.edu

http://www.bioscience.org/current/vol13.htm